24TH International Free Electron Laser Conference & 9th FEL Users Workshop
ARGONNE, ILLINOIS USA, SEPTEMBER 9-13, 2002

ADVANCED PHOTOCATHODE SIMULATION AND THEORY

Kevin L. Jensen†, Patrick G. O'Shea, Donald W. Feldman

Inst. for Res. in Electronics and Applied Physics

U. Maryland, College Park, MD 20742

POSTER SESSION TU-P-13

This work supported by The Joint Technology Office/Office of Naval Research and The Naval Research Laboratory

† *Permanent Address: Code 6841, ESTD, Naval Research Laboratory, Washington, DC 20375-5347*

ABSTRACT

A low work function dispenser type photocathode that is self-annealing or repairing would have a substantial impact on Free Electron Lasers (FEL's). On such a cathode, the emitting surface is constantly renewed by replenishment of low-work-function material. A photo-dispenser cathode should operate at a relatively low temperature compared to a conventional dispenser cathode (but higher than a metal photo-cathode to improve lifetime), and is anticipated to be robust and long-lived. Coatings cause a reduction in the transport barrier experienced by the electrons through a complex modification of the potential at the surface, e.g., a reduction in work function due to dipole effects. In this work, we address several such theoretical components in the theory and simulation of advanced photocathodes as part of a program, concurrent with experimental efforts [1], to develop dispenser cathodes for use in high power rf photoinjectors. Issues in a theoretical description of the emission process include: the nature of the energy distribution of the photo-excited electrons (used, e.g., in beam formation and emittance growth simulations); methods to model emission; the dependence of the emitted current on coverage, the nature of the low work function coating (and its effects on the emission barrier); and environmental conditions such as background pressure and operational temperature. Developments in and the status of these emission models will be the subject of the present work.

SEE ALSO: (TU-P-09)

"Experimental Studies of Advanced Photocathodes" D. W. Feldman, P. G. O'Shea, K. L. Jensen, M. Virgo

OUTLINE

PART A: TRANSMISSION COEFFICIENTS AND A THERMAL-FIELD EQ.

3-7

- FN-RLD Theory Update: for Photoemission Near the Barrier Maximum, Approximations Used for the Transmission Coefficient, As Developed for the Fn and Rld Equations, Break Down. A Hyperbolic-Tanh Approximation to T(E) Is Developed, Which Can Be Used to Give a Generalized Thermal Field Equation.

PART B: A MODEL OF PHOTOEMISSION FROM A TUNGSTEN TIP

8-12

- Using T(E) Developed Above, the Analysis of the Expected Quantum Efficiency From a Laser-illuminated Tungsten Tip Is Evaluated. A Description of the Geometrical Model of a Tungsten Wire Is Provided. The Methodology of Evaluating the QE Estimate Is Developed.

PART C: TOWARDS A MODEL OF THE DIPOLE LAYER: THE WIGNER FUNCTION APPROACH

13-19

- Coatings (e.g., Ba) bring Φ down By Modifying the Surface Barrier (Work Function Lowering). Phenomenological Theories Relating Coverage to Φ Do Not Treat the Barrier Shape. An Overview of Methodology Being Developed to Analyze the Barrier and Dipole, Using a Wigner Function Approach to Emission Including Many-body and Electron Density Variation Effects, Is Given.

THE FN, RLD, & WKB APPROXIMATIONS

The Fowler Nordheim (FN) and Richardson-Laue-Dushman (RLD) Eqs. Dependent upon $T_{wkb}(E)$

$$T_{WKB}(E) = \exp\{-2\theta(E)\}$$

$$\theta(E) = \frac{2}{\hbar}\sqrt{2mFL^3}\,R\left(\frac{x_-}{L}\right); R(s) = \int_0^\infty \frac{\cos^2(\varphi)\sin^2(\varphi)}{\sqrt{s+\sin^2(\varphi)}}\,d\varphi$$

$$J(F,T) = \frac{1}{2\pi}\int_0^\infty \left(\frac{\hbar k}{m}\right) T(E(k))\, f(E(k))\, dk$$

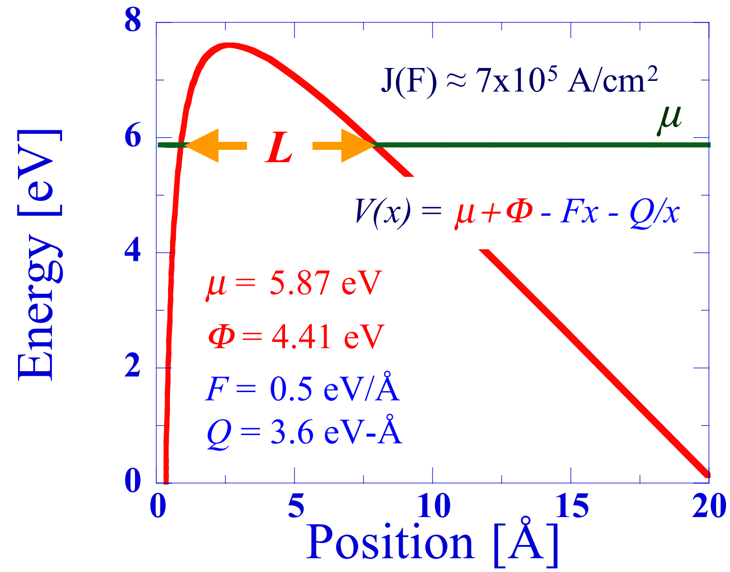

FN: Emission Near E=μ Dominates, and Supply Function *f(E)* is "Cold"

$$-\ln(T(E)) \approx \frac{b_{fn}}{F} + c_{fn}(\mu - E); f(E) = \frac{m}{\pi\hbar^2}(\mu - E)$$

$$b_{fn}(F) = \frac{4}{3\hbar}\sqrt{2m\Phi^3}\,v(y); \quad c_{fn}(F) = \frac{2}{\hbar F}\sqrt{2m\Phi}\,t(y)$$

$$J_{FN}(F) = a_{fn}F^2 \exp\left(-\frac{b_{fn}}{F}\right)$$

$$a_{fn} = \frac{1.5414\times10^{-6}\,A/eV}{\Phi t(y)^2}; b_{fn} = \left(6.8309\times10^7\,\frac{eV}{cm}\right)\Phi^{3/2}v(y)$$

RLD: Emission Over Barrier Dominates, and Supply Function *f(E)* is "Hot"

$$T(E) = \Theta\left[E - \left(\mu + \Phi - \sqrt{4QF}\right)\right]$$

$$f(E) = \frac{m}{\pi\hbar^2}\exp[\beta(\mu - E)]$$

$$J_{RLD}(F) = A(T[K])^2 \exp\left(-\frac{B}{T}\right)$$

$$A = 120.17\,\frac{Amp}{cm^2K^2}; B = 11604.5K(\Phi[eV])$$

T(E) SYNTHESIS & TANH-T(E) MODEL

Airy and WKB Synthesis

$$T(E) = \frac{C(k)}{1 + \exp\left[2\theta\left(E(k)\right)\right]}$$

$$C(k) = \frac{64k^6 x_-^4}{\frac{2m}{\hbar^2}F^2\left(x_0^2 - x_-^2\right)^2 + 64k^6 x_-^4}$$

$$\theta(E > E_o) = \theta(E_o) + \left(\partial_E \theta(E_o)\right)\left(E - E_o\right)$$

x_o = Barrier Maximum
$x_\pm$ = Zeros of $V(x)-E$
$E_o = \mu + \Phi - 2.5\sqrt{(QF)}$

T(E) Suggests a Tanh-Approximation

$$T(E) \approx \frac{T_o}{1 + \exp\left[b\left(E_c - E\right)\right]}$$

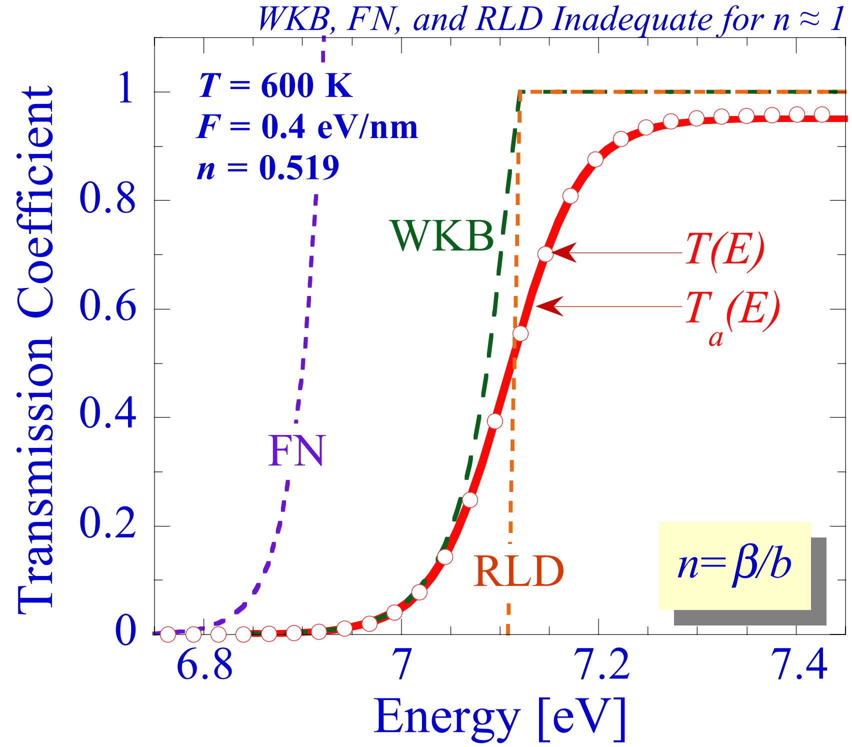

FN-based Approximation (T's evaluated at $E = E_m$)

$$T_o = \left[\frac{2(T')^2 - TT''}{(T')^2 - TT''}\right]T; \quad b = 2\frac{(T')^2 - TT''}{TT'}$$

$$E_c = E_m - \frac{TT'}{2(T')^2 - TT''}\ln\left(1 - \frac{TT''}{(T')^2}\right)$$

$$E_c \approx \begin{cases} \left(\mu + \dfrac{b_{fn}}{c_{fn}F}\right) & n > 1 \\ \mu + \Phi - \sqrt{4QF} & n < 0 \end{cases}$$

$$E_m \approx E_c - \frac{1}{b}\begin{cases} -\ln\left(\dfrac{1}{n} - 1\right) & \{n < 1\} \\ b\left(E_c - \mu\right) + \dfrac{n - e^{-n}}{n\left(1 + e^{-n}\right)} & \{n > 1\} \end{cases}$$

E_c ESTIMATION & E_m BEHAVIOR

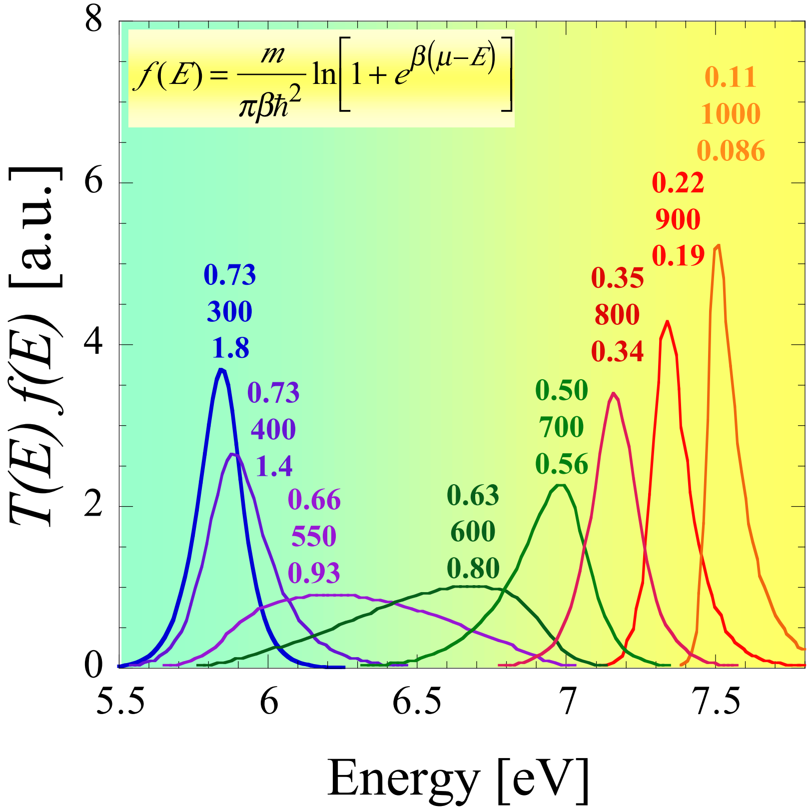

Evolution of *J(F,T)* @ 1 A/cm² (Φ = 2.0 eV)

Top #:	Field [V/nm]
Middle #:	Temp [K]
Bottom #:	$n = \beta/b$

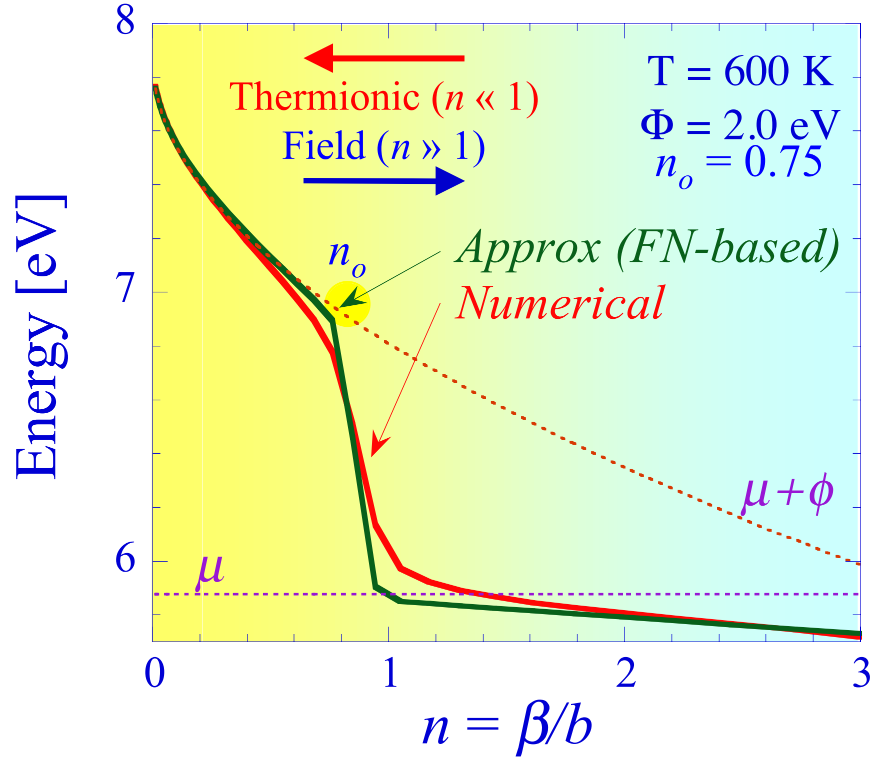

Compared to a Numerical Search for E_m (e.g., By Bisection), the Zeroth Order + Correction Approach Adequately Estimates Its Location Using the FN Estimate to b

$$b(F,\Phi)\big|_{FN} \approx c_{fn} = \frac{\sqrt{2m\Phi}}{\hbar F}t(y)$$

GENERALIZED *J(F,T)* EQUATION

Using the Tanh-form Best Fit of *T(E)*:

$$J(F,T) = \frac{qm}{2\pi^2\hbar^3}\left(\frac{T_o}{\beta^2}\right)\left\{\int_{-\infty}^{b\mu+p}\left[\frac{\ln\left[1+e^{n(x-p)}\right]}{e^x+1}\right]dx\right\}$$

$$= \frac{qm}{2\pi^2\hbar^3}\left(\frac{T_o}{\beta^2}\right)N(-\infty, b\mu+p)$$

Nomenclature:

$T(E) \approx T_o / \{1+\exp[b(E_c-E)]\}$

$x = b(E_c - E)$

$p = b(E_c - \mu)$

$n = \beta/b$

x_p, λ, N_g: Integrand Approximated By Gaussian of Form $N_g \exp[-\lambda(x-x_p)^2]$

Separate *N* Into 3 Integration Regions:

- Field: $N_A = N(p, b\mu+p)$
- Intermediate: $N_B = N(-b\phi+p, p)$
- Thermal: $N_C = N(-\infty, -b\phi+p)$
- FN: $n = \infty$ limit of N_A
- RLD: $n = 0$ limit of N_C

$$N_A = \frac{n\left[(n+1)n+1\right]}{n+1}e^{-p}$$

$$N_B = \frac{n}{2}\sqrt{\frac{\pi}{\lambda}}N_g\left\{Erf\left[\sqrt{\lambda}\left(b\phi - x_p\right)\right] - Erf\left[\sqrt{\lambda}x_p\right]\right\}$$

$$N_C = \left(1 - \frac{ne^{p-b\phi}}{n+1}\right)e^{-bn\phi}$$

ANALYTICAL IMAGE CHARGE MODEL

Simple Model: A Triangular Potential Barrier

$$V(x) = V_o - Fx = \frac{\hbar^2}{2m}\left(k_o^2 - fx\right)$$

Schrödinger's Eq. Solution (Leading Order)

$$y(x) = \exp\left(ikx\right) + r(k)\exp\left[-ik\left(x - k_o^{-1}\right)x\right]$$

- ***ρ(x)*** **affected Mostly by Barrier Height, Less by Details for "Abrupt" Potentials:** Effects of a Change in Barrier Height Result in a Shift in Electron Density - Less by a Change in Shape

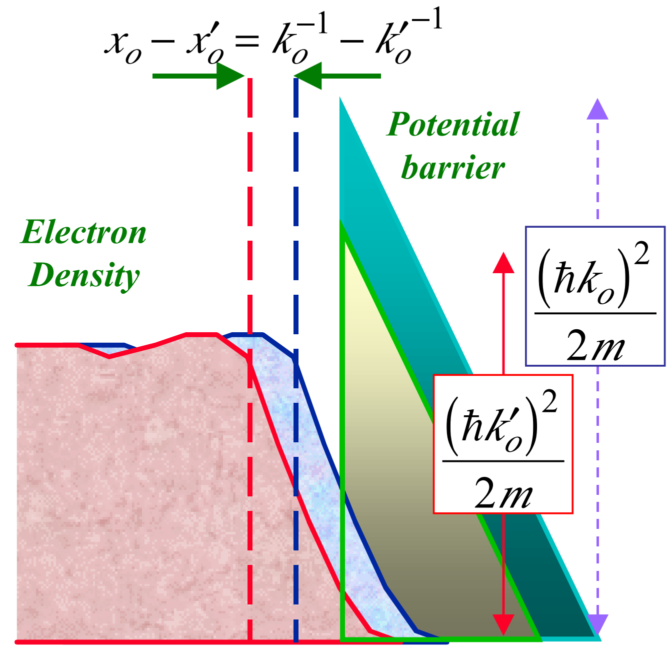

$$V_{analytic}(x>0) = \mu(T) + \Phi_o(T) + \frac{8}{3\pi}Qk_F^3x_i^2 - F(x - x_o) - \frac{Q}{x + x_o}$$

Barrier Height

$$k_F x_o \equiv \lambda = \left(\frac{\mu}{V_{\max}}\right)^{1/2}$$

Charge Neutrality

$$k_F x_i \approx \frac{84\lambda \ln\left(\frac{17}{25}\left(k_F x_o\right)^2\right)}{168 - 36\left(k_F x_o\right)^2 + 5\left(k_F x_o\right)^4}$$

SIMPLE MODEL OF 3-D

A Line of Uniform Charge Per Unit Length Gives Rise to Ellipsoidal Equipotential Lines and May Be Used to Model Apex Fields

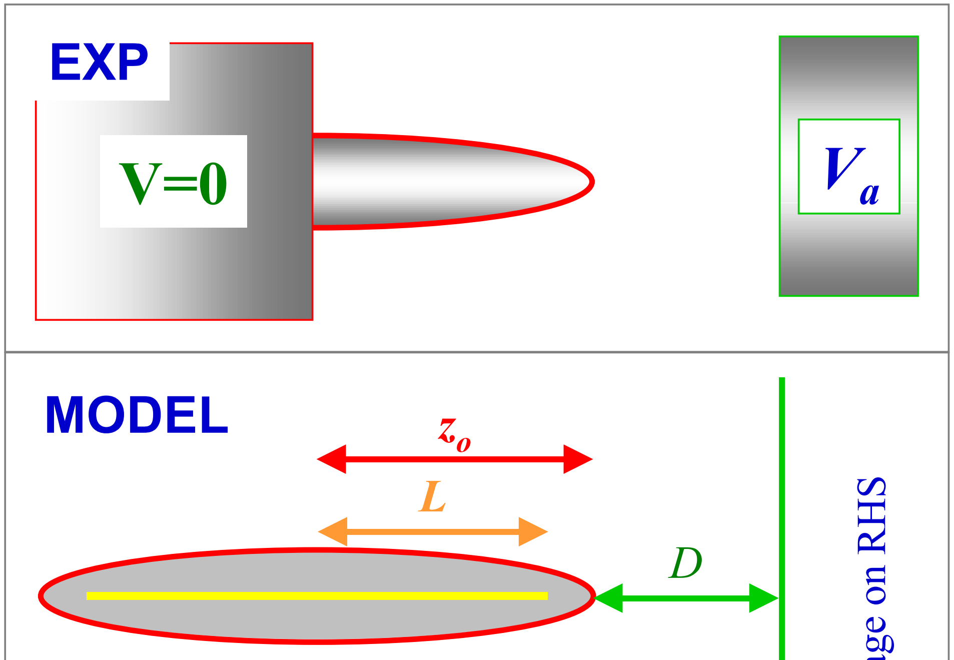

Charge Per Unit Length Chosen to Give $V = 0$ at $z = L$, Apex Radius a_s, and $V = V_a$ at $z = z_o + D$

Potential Due to Line Charge

$$V(\rho, z) = 2V_o \left\{ \frac{Q_0\left(\frac{u(\rho,z)}{L}\right) - Q_0\left(\frac{z_o}{L}\right)}{Q_0\left(\frac{D+z_o}{L}\right) - Q_0\left(\frac{z_o}{L}\right)} \right\}$$

$$u(\rho, z) = \frac{1}{2}\left[\sqrt{\rho^2 + (z+L)^2} + \sqrt{\rho^2 + (z-L)^2}\right]$$

Field At Apex of Ellipsoid:

$$F_{tip} = \partial_z V(\rho = 0, z = z_o)$$
$$= \frac{L}{a_s z_o}\left(Q_0\left(\frac{D+z_o}{L}\right) - Q_0\left(\frac{z_o}{L}\right)\right)^{-1} V_a$$

Relations

$$L = \sqrt{z_o(z_o - a_s)}$$

$$Q_0(x) = \frac{1}{2}\ln\left[\frac{x+1}{x-1}\right]$$

ELLIPSOIDAL FIELD VARIATION

Prolate Spheroidal Coordinate System Allows for Exact Solution of Ellipsoid in a Background Field in Terms of Legendre Polynomials. **Field Variation** Along Emitter Surface Can Then Be Obtained.

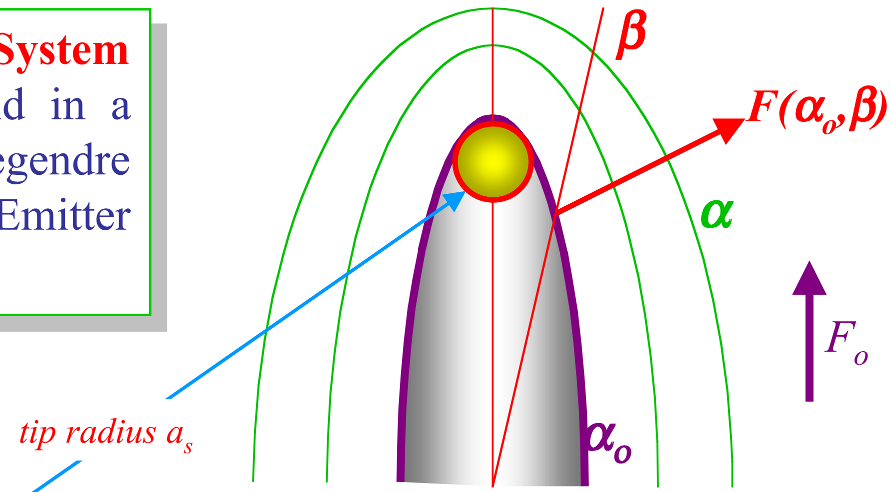

Prolate Spheroidal Coordinates

$$z = \frac{1}{2} a_h \cosh(\alpha)\cos(\beta)$$

$$\rho = \frac{1}{2} a_h \sinh(\alpha)\sin(\beta)$$

$$a_h = \frac{2\cosh(\alpha)}{\sinh^2(\alpha)} a_s$$

Gradient to Evaluate $F(\alpha,\beta)$

$$\hat{\alpha}\cdot\vec{\nabla} = \frac{1}{\sqrt{(\partial_\alpha x)^2 + (\partial_\alpha y)^2 + (\partial_\alpha z)^2}} \frac{\partial}{\partial\alpha}$$

$$= \frac{2}{a_h}\left[\sin^2(\beta) + \sinh^2(\alpha)\right]^{-1/2} \frac{\partial}{\partial\alpha}$$

Potential in Ellipsoidal Coordinates

$$V(\alpha,\beta) = F_o z(\alpha,\beta)\left\{\frac{Q_1(\cosh(\alpha))}{Q_1(\cosh(\alpha_o))} - \frac{\cosh(\alpha)}{\cosh(\alpha_o)}\right\}$$

$$F_{tip} = \partial_z V(\alpha,0) = -\frac{F_o}{\sinh^2(\alpha_o) Q_1(\cosh(\alpha_o))}$$

$$F(\alpha_o,\beta) = \frac{\sinh(\alpha_o)\cos(\beta)}{\sqrt{\sinh^2(\alpha_o) + \sin^2(\beta)}} F_{tip}$$

FN QUANTUM EFFICIENCY (1-D)

Thermal 1-D Fermi Dirac Distribution

Integrated Over Momentum Perpendicular to the Surface

$$f\left(E(k)\right) = \frac{m}{\pi\beta\hbar^2}\ln\left\{1+\exp\left[\beta\left(\mu - E(k)\right)\right]\right\}$$

$$\phi = \Phi - \sqrt{4QF}$$
$$= (1-y)\Phi$$

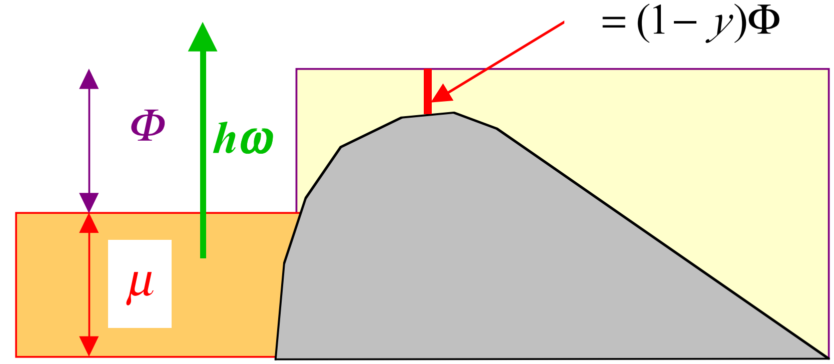

FN Version of Tanh-T(E) Approximation

$$T(E) = T_o\left\{1+\exp\left[\frac{b_{fn}}{F} + c_{fn}\left(\mu - E\right)\right]\right\}^{-1}$$

e⁻ Out Per Unit Time Per Unit Area In 3-step Emission Model Is Current Density

$$J_\omega(F) = \frac{q}{2\pi}\int_0^\infty \left(\frac{\hbar k}{m}\right) T\left(E(k)+\hbar\omega\right) f\left(k\right) dk$$

For a Planar Surface, Ratio of 1-D J(F) Approximates **QE**

compare to Eq. 7 of R. H. Fowler, PRB38, 45 (1931)

$$\frac{\int_0^\infty T(E+\hbar\omega) f(E)\,dE}{\int_0^\infty f(E)\,dE} = T_o \frac{\left\{\left(\hbar\omega - \frac{2v(y)}{3t(y)}\Phi\right)^2 + \frac{1}{2m\Phi}\left(\frac{\hbar F}{\mu t(y)}\right)^2\right\}\beta^2 + \frac{1}{6}\pi^2 + 2}{(\beta\mu)^2 + \frac{1}{6}\pi^2 + 2}$$

FN Conditions: Relation Valid when $\beta / c_{fn} > 1$

QUANTUM EFFICIENCY (3-D)

Generalize the 1-D Result:

- **Integrate Product of J*dΩ Over Surface**
- **Evaluate Ratios Numerically Using tanh-T(E)**
- **Use Analytical Image Charge**

$$QE = \frac{\int_{\Omega} d\Omega \int_0^{\infty} dE\, f(E)\, T\left[E+\hbar\omega; F(\rho,z)\right]}{\int_{\Omega} d\Omega \int_0^{\infty} dE\, f(E)}$$

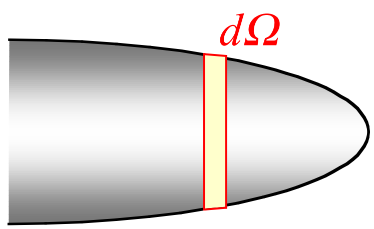

T	= 1000 K
Φ	= 4.6 eV
ρ	= 1.26E23#/cm^3
L	= 1.0 mm
D	= 2.5 mm
a_s	= 1.1 μm

$$d\Omega(\rho,z) = 2\pi\rho\sqrt{\left(\partial_\beta \rho\right)^2 + \left(\partial_\beta z\right)^2}\, d\beta$$
$$= 2\pi a_s^2 \sin(\beta)\frac{\cosh^2(\alpha)}{\sinh^3(\alpha)}\sqrt{\sinh^2(\alpha)+\sin^2(\beta)}\, d\beta$$

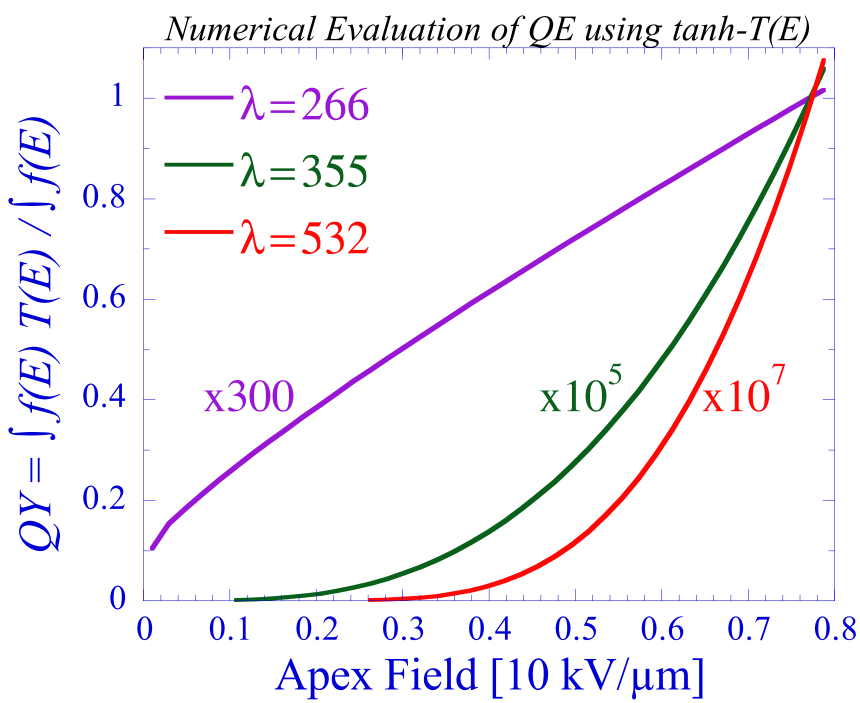

Asymptotic Formula w/ FN parameters in tanh-T(E) shows non-linearity on an FN plot of J(F)

$$\frac{1}{2\pi\hbar}\int_0^{\infty} dE\, f(E)\, T\left[E+\hbar\omega\right] \approx \frac{9qm}{36\pi^2\hbar^3}\left(\hbar\omega - \frac{2v(y)}{3t(y)}\Phi\right)^2$$

EMISSION BARRIER

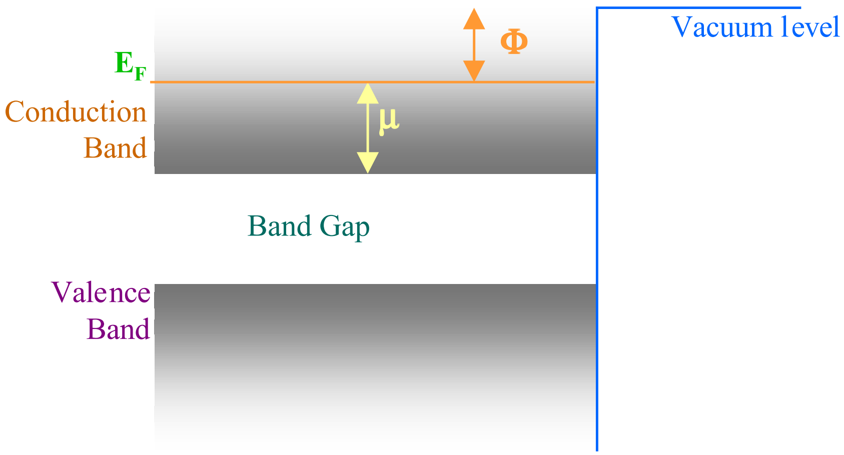

$$V_o = -\frac{\partial}{\partial \rho}\left[\rho \varepsilon_{xc}(\rho)\right] - \Delta\phi + \varepsilon_{ion}$$

Exchange Correlation Potential

Dipole Term

Ionic Core

EMISSION FROM METALS

Large Density of Electrons Exist In Conduction Band (> 60 Billion / μm^3);

Very Small Fraction Contribute to Current ($A/cm^2 \approx 62$ per μs per μm^2)

The Largest Component of the Barrier Is Due to the Exchange Correlation Potential

EXCHANGE-CORRELATION POTENTIAL

The Density ρ of an Electron Gas Is

$$\rho = \frac{2}{(2\pi)^3}\int_0^\infty f_{FD}\big(E(k)\big)d^3k = \frac{k_F^3}{3\pi^2}$$

Kinetic Energy

$$\varepsilon_{ke} = \frac{2}{(2\pi)^3}\int_0^\infty \frac{(\hbar k)^2}{2m} f_{FD}\big(E(k)\big)d^3k = \frac{3}{5}\,\mu\rho$$

$$V_{xc}(x) = -\frac{\partial}{\partial\rho}\left[\rho\left(\varepsilon_{ex} + \varepsilon_{corr}\right)\right]$$

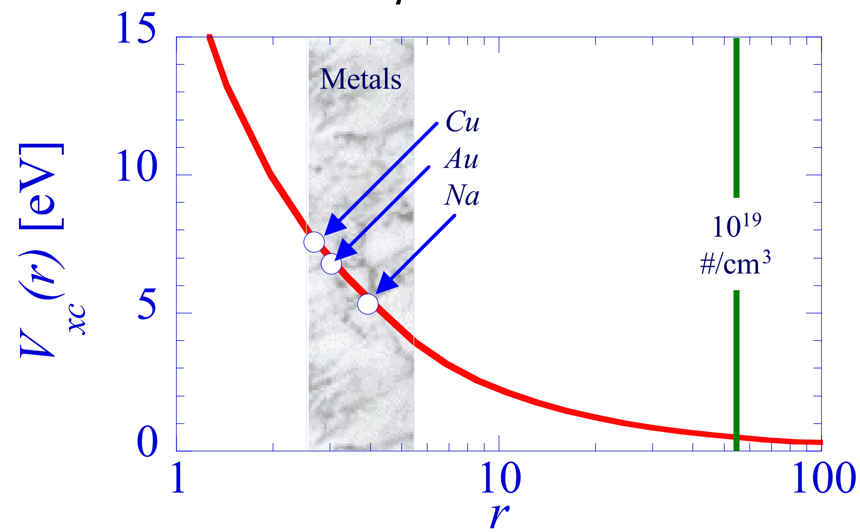

Exchange (Potential) Energy

$$\varepsilon_{ex} = \frac{2}{(2\pi)^3}\int_0^\infty f_{FD}(E)v_q(k_F)d^3k = -\frac{3}{4}Q\left(\frac{3\rho}{\pi}\right)^{1/3}$$

$$v_q(k_F) = \int \frac{2Q}{q^2}\theta\left(k_F - \left|\vec{k} + \vec{q}\right|\right)d^3q$$

Correlation (Potential) Energy - *Wigner*

$$\varepsilon_{corr} = -\frac{2Q}{a_o}\left(\frac{0.876}{r + 7.811}\right)$$

$$\rho(r) = \frac{3}{4\pi(ra_o)^3}$$

A MODEL OF BARRIER PENETRATION

STEP-FUNCTION BARRIER

Origin (x_i) Of + Background Differs From That Of Electrons ($x = 0$) To Preserve Global Charge Neutrality

Simple Model of Effect for Step Function Potential Barrier and Plane Wave Solutions to the Electron Wave Function

$$0 = \int_{-\infty}^{\infty} \{\rho_e(x) - \rho_i(x)\} dx$$

Electrons $\rho_e(x) = \frac{1}{2\pi} \int_0^\infty f(k) |\psi_k(x)|^2 dk$

Ion cores $\rho_i(x) = \rho_o \theta(x - x_i)$

Electron Density Can Be Approximated by a Hyperbolic-tangent From Matching $\rho(x_i)$, $\partial_x \rho(x_i)$

$$\rho_e(x) \approx \frac{\rho_o}{2} \{1 - \tanh[\lambda k_F (x - x_i)]\}$$

$$\lambda \approx \frac{5}{8}; \quad x_i \approx x_o - \frac{5}{2k_F}$$

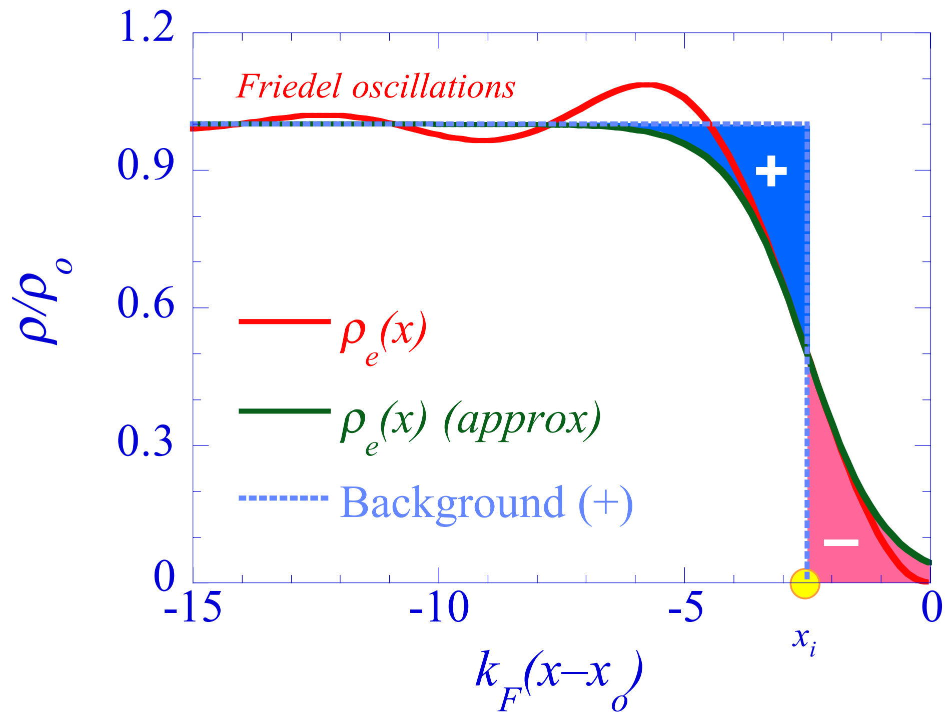

Magnitude of Dipole

(Tanh-model: Qualitative, Overestimates Magnitude)

$$\Delta\phi = q^2 \frac{\rho_o}{\varepsilon_o} \left(\frac{1}{4\lambda^2 k_F^2} \right) \int_0^1 \frac{\ln(u)}{1+u} du = -\frac{64\pi}{225} Q k_F$$

Many-body Effects (Ex-Corr Potential) Dependent Upon Variation In Electron Density Not Accounted for by This Model

THE WIGNER FUNCTION APPROACH

The Wigner Function Is a Quantum Distribution Function Satisfying an Equation Similar to Boltmann's Transport Equation (BTE), but Includes Effects Due to Tunneling.

General and

Collisionless Steady State

$$i\hbar\cancel{\frac{\partial}{\partial t}} = -\frac{\hbar k}{m}\frac{\partial}{\partial x} f(x,k;t) + \int_{-\infty}^{\infty} V(x,k-k') f(x,k';t)\,dk' + \cancel{\partial_{coll} f}$$

$$V(x,k) = \frac{1}{\pi\hbar}\int_{\pm\infty}^{\infty}\left[V(x+y) - V(x-y)\right]\sin(2yk)\,dy$$

Example: Gaussian Potential Profile
$V(x) = V_o \exp[-ax^2]$

$$V(x,k) = -\frac{2V_o}{\pi\hbar}\left(\frac{\pi}{a}\right)^{1/2}\exp\left[-k^2/a\right]\sin(2kx)$$

For $a \ll 1$ & $k' = k+s$, Expand $f(x,k+s)$

$$f(x,k+s) \approx f(x,k) + s\partial_k f(x,k)$$

Integral over $V(x,k)$ drops symmetric $f(x,k)$, keeps anti-symmetric $s\partial_k f$, giving BTE

$$0 = -\frac{\hbar k}{m}\partial_x f(x,k) + \frac{1}{\hbar}\partial_x V(x)\partial_k f(x,k)$$

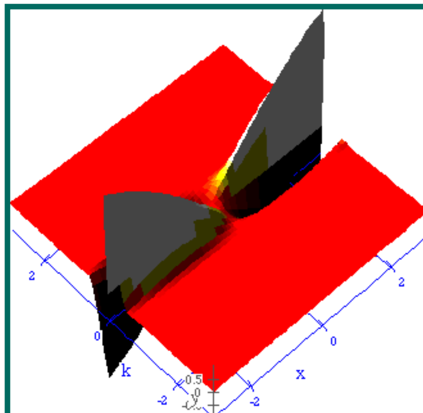

Large a: Potential Is Very Broad; $V(x,k)$ Tends to Examine Local k Changes in Distribution Function Transitions to BTE

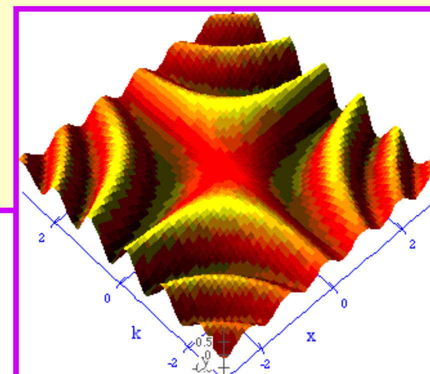

Small a: Potential Is Very Sharp; $V(x,k)$ Tends to Examine Broad Regions of Distribution Function Accounts for Tunneling

DISCRETE VERSION OF WDF DIFF. EQ.

The numerical solution of the WDF integro-differential equation generally requires upwind-downwind second order differencing algorithms which account for incoming boundaries for $k > 0$ (LHS) and $k < 0$ (RHS), necessitating a large sparse-matrix solution. However, for photoemission conditions, it is the case that in the absence of excitation, no tunneling transmission occurs and all electrons are reflected. **Consequently, *f(x,–k) = f(x,k)*.** This allows for a vastly lower memory approach as well as the inclusion of the $k = 0$ momentum value which is normally excluded but which has important consequences. The price is small accumulating numerical errors.

$$0 = -\left(\frac{\hbar^2 \Delta k}{m\Delta x}\right) j\hat{\Delta} F_j(x) + \frac{1}{\pi}\sum_{j'=-N/2}^{N/2} S(j-j')F_{j'}(x)$$

$$S(J) = \frac{1}{N}\sum_{i=-N/2}^{N/2} \Delta V_l(x)\sin\left(lJ\frac{2\pi}{N}\right)$$

$\boldsymbol{k \neq 0}$

$$0 = -\left(\frac{\hbar^2 \Delta k}{m\Delta x}\right) \hat{\Delta} F_j(x) + \frac{1}{\pi}\sum_{j'=-N/2}^{N/2} C(j')F_{j'}(x)$$

$$C(j') = \frac{1}{N}\sum_{l=-N/2}^{N/2} l\Delta V_l(x)\cos\left(lj'\frac{2\pi}{N}\right)$$

$\boldsymbol{k = 0}$

Discretization of variables

- $k(j) = j\Delta k; \quad y(l) = l\Delta x$
- $f(x,k) = F_j(x)$
- $\Delta V_l(x) = V(x+l\Delta y) - V(x-l\Delta y)$

DIFFERENCING OPERATOR
Second-order accurate scheme

$$\hat{D}\bullet \Delta\vec{F}(x) + \hat{M}(x)\bullet\vec{F}(x) = 0 \Rightarrow$$

$$\left[\hat{D} + \frac{1}{2}\hat{M}(x+\Delta x)\right]\bullet\vec{F}(x+\Delta x) = \left[\hat{D} - \frac{1}{2}\hat{M}(x)\right]\bullet\vec{F}(x)$$

HYPERBOLIC DENSITY APPROXIMATION

Effects from an abrupt boundary can extend far into metal where variations are minor and compromise numerical methods. An approach is to use a non-uniform discretization in x so that where the potential is smooth (further away from the origin) the separation between adjacent points increases so that a coarse grid is used, but near the origin where the potential is rapidly varying, a fine grid is used. An analytical approximation to the potential (and by virtue of the Exchange-Correlation Potential, the density) must be used. We employ the TANH approximation to density, where the parameters are extracted from the numerical solution of the WDF, thereby maximizing correspondence.

α and x_i are numerically evaluated from the discrete *Fj(x)*. *ϕ(x)* is added to the Exchange Correlation potential to construct *V(x)*. Multiple iterations ensure solution is consistent.

$$\rho(x) = \frac{\rho_o}{\left[1+\exp\left(\alpha(x-x_i)\right)\right]}$$

$$\phi(x) = \frac{\rho_o}{\alpha^2\varepsilon_o} = \begin{cases} \displaystyle\int_0^{\exp\left(\alpha(x-x_i)\right)} \left(\frac{1}{u}\right)\ln\left(1+u\right)du & x \le x_i \\ \displaystyle\frac{\pi^2}{12} + \int_{\exp\left(-\alpha(x-x_i)\right)}^{1} \left(\frac{1}{u}\right)\ln\left(1+u\right)du & x > x_i \end{cases}$$

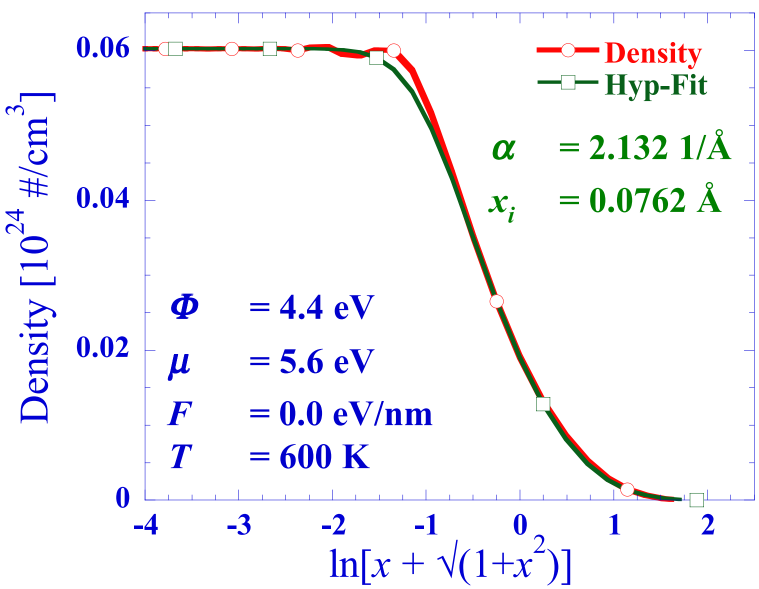

Red line: Numerical (evaluation of WDF)
Blue line: Best Hyperbolic fit

NUMERICAL RESULTS OF WDF

Preliminary results show viability of method to extract the Exchange-Correlation, electron dipole, and ion potential from the WDF. Parameters are for Tungsten. The effects of the addition of a dipole term arising from coatings (e.g., Ba) modify the form of *V(x)*. The results of these simulations shall be shown in a separate work.

Spacing Algorithm (Δx_o = 0.2 Å; C = 2.0, N = 45)
Maximum x = 1.12 nm; Minimum x = –7.3 nm

$$x(i) = (i - N)\left[\Delta x_o + C\left(\frac{i - N}{N}\right)^2\right]$$

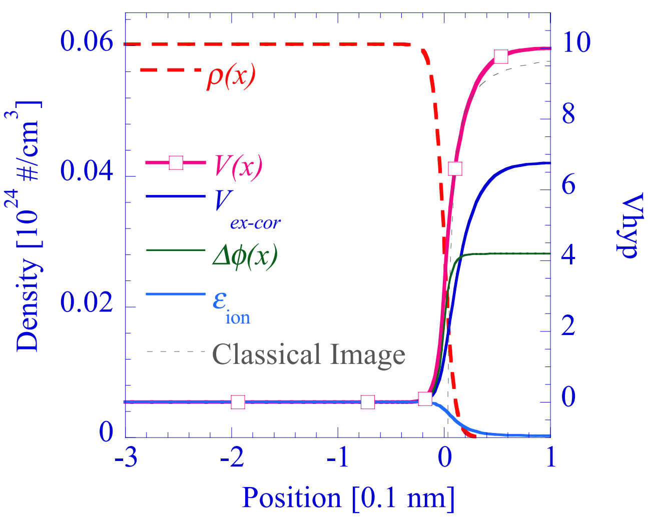

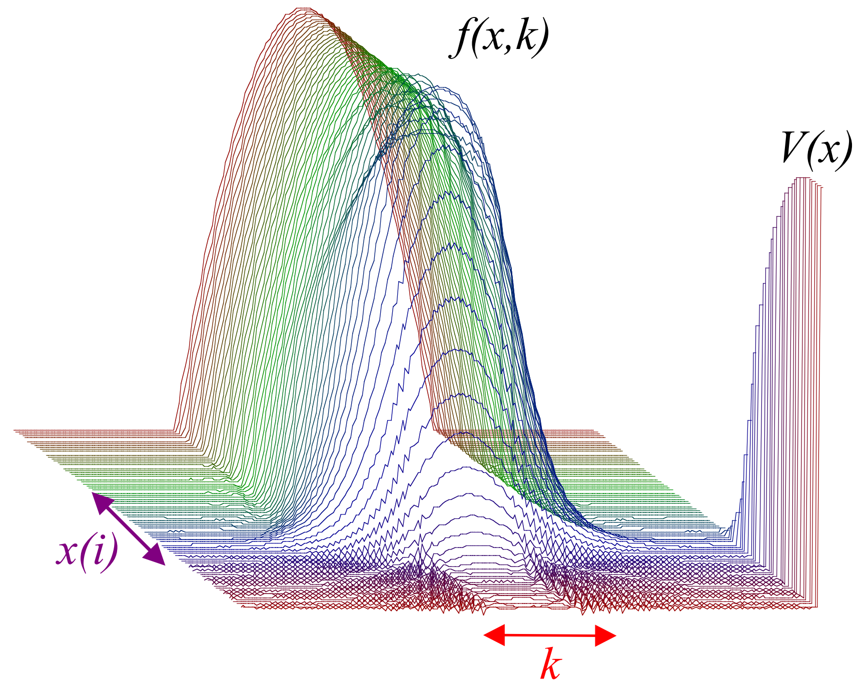

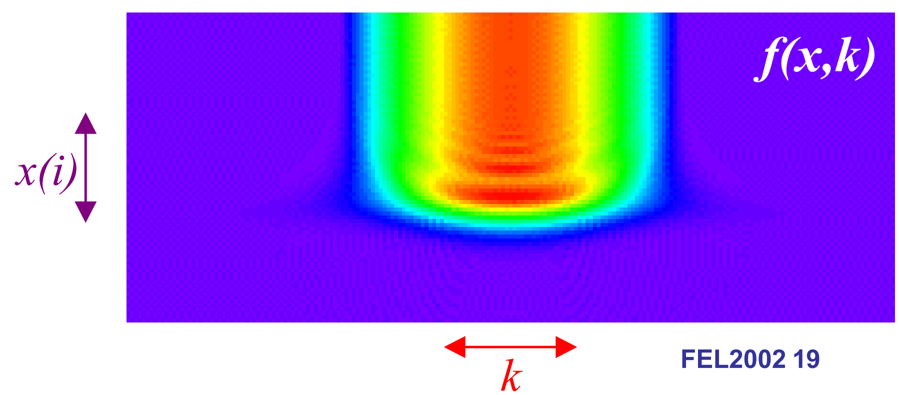

SUMMARY

Part A: Transmission Coefficients And A Thermal-field Eq.

- **A TANH Model of the Transmission Coefficient Was Developed Based on an Analysis of Tunneling and Thermionic Emission Phenomena.**
- **A Generalized Thermal Field Emission Equation Was Given.**

Part B: A Model Of Photoemission From A Tungsten Tip

- **The Transmission Coefficient From Part A Was Used, Along With the Analytical Image Charge Approximation, to Estimate Quantum Efficiency From an Illuminated Tungsten Wire. Approximation Formulae Are Given. Numerical Results Were Obtained for the Case of a Rotationally Symmetric Ellipsoidal Wire. Precipitous Drop-off As a Function of Photon Wavelength Observed.**

Part C: Towards A Model Of The Dipole Layer: The Wigner Function Approach

- **Methodology for Generating the WDF for the Emission Barrier Under Assumption That Non-photoemission Current Was Negligible Was Given. Relied on Symmetry of the Distribution Function Associated With Non-emission, Thereby Allowing the k=0 Component to Be Included. Designed to Allow for Coating Modifications.**
- **Electron Density Variation Strongly Resembles a TANH Function and Allows for a Discretization Alogorithm Which Extends Far Into the Bulk.**